Femtosecond Pulse Propagation in a Highly Nonlinear Photonic Crystal Fiber

J. F. Gabayno[1], C. A. Alonzo[2], and W. O. Garcia[3]
National Institute of Physics, University of the Philippines,
Diliman, Quezon City 1101
E-mail: [1]jgabayno@nip.upd.edu.ph; [2]cca@nip.upd.edu.ph;
[3]wgarcia@nip.upd.edu.ph

ABSTRACT

Femtosecond pulses are launched into a highly nonlinear photonic crystal fiber (PCF). The input and output spectra were measured using a monochromator and streak camera. The spectrum of the output from a 50 cm PCF pumped at 794 nm for different pump powers features asymmetric side lobes due to intrapulse Raman scattering. Similar measurements on a 100 cm PCF pumped at 795 nm highlight the appearance of blueshifted peaks as a result of energy transfer of solitons to dispersive waves. Broadening in the spectrum is observed and attributed to Raman-scattering-induced soliton self-frequency shift. Spectrograms of both input and output pulses into a 50 cm PCF are captured using a streak camera. The spectrum reveals that individual modes observed on the spectrogram are actually a decomposition of the input pulse.

INTRODUCTION

Highly nonlinear photonic crystal fiber (PCF) is a new type of microstructure material that is now drawing the interest of researchers working in the areas of spectroscopy and telecommunication. Just recently, application of these materials with ultrafast laser sources such as those in the femtosecond regime had productively set a new trend on supercontinuum generation (SCG). Ultimately, the coherent broadband produced through SCG will find application such as a light source for telecommunication's WDM systems. On the other hand, as far as the basic research is concerned PCFs are attractive media for studies related to understanding the complexities of nonlinear processes. Currently, customizing the structure of PCFs to increase its nonlinear properties has become a standard procedure during fabrication. This liberty has not been previously available with conventional fibers. Even the dispersion of PCFs can be designed so that it could exhibit zero-dispersion wavelengths (ZDWs) that are within the visible range. As a result, PCF could well be integrated into transmission systems which require less dispersion-induced pulse broadening.

The structure of conventional fibers is primarily divided into a core with a higher refractive index than the surrounding cladding. An incident light into this fiber is effectively guided inside the core only if its angle of incidence satisfies the condition imposed by Snell's law. Efficient coupling of the incident light strongly depends on the mismatch in the indices of refraction between core and cladding. To address this requirement, dopants are mixed with the core material during fabrication. The inclusion of dopants increases the refractive index difference on the core-cladding boundaries. In highly nonlinear PCFs, however, an array of air-silica cladding compensates for the high index difference with the core, which is made up of pure silica. The cladding, as a result of the air holes and silica matrix, has a very low effective index. Effectively, incident light is confined inside the core due to total internal reflection (TIR).

These properties of solid-core PCFs, e.g., high index mismatch of core and cladding, and tailored core diameter and ZDW permit several nonlinear processes during light propagation. Worth mentioning are the stimulated Raman scattering (SRS), self-phase modulation (SPM), and four-wave mixing (FWM), all of which are principal factors towards SCG.

In this paper, we present our results on the propagation of femtosecond pulses inside a solid-core PCF. We investigated the spectra of the input and output pulses with different input pump powers. The pump wavelength used is very close to the ZDW of the PCF. The spectrum from 50 and 100 cm PCFs is measured using a spectrometer and a streak camera.

EXPERIMENT SETUP

The PCF is pumped at 795 nm with a mode-locked Ti: Sapphire laser (Tsunami) producing ~100 fs pulses extending over the near-infrared region from 705 to 985 nm and operating at 82 MHz repetition rate (Fig. 1).

A Glan-laser prism polarizes the pulses from the femtosecond laser. It also provides an easy control over the amount of pump power launched into the PCF.

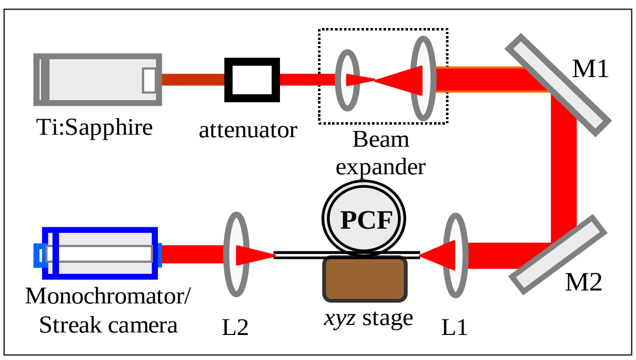

Fig. 1. A diagram of the setup reveals a beam of femtosecond pulses emanating from a Ti:Sapphire laser. The beam is attenuated by a Glan-laser polarizer and expanded to a diameter of 4 mm. Two mirrors M1 and M2 steer the collimated beam towards lens L1; L1 and L2 couple the pulses in and out of the photonic crystal fiber (PCF). The PCF is attached to an *xyz*-flexure stage for efficient and easy positioning. The spectral profiles of the output pulse were detected and captured using a monochromator and streak camera, respectively.

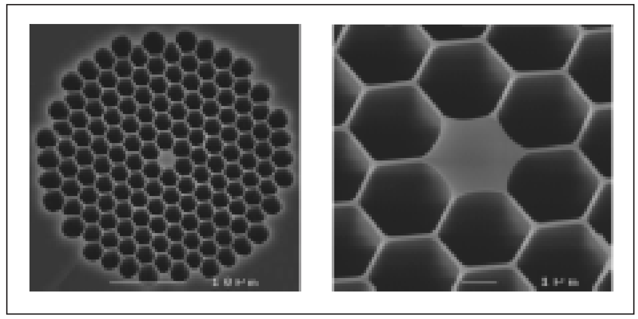

Fig. 2. Scanning electron micrograph (SEM) photos of an (a) array of air-silica cladding and (b) pure silica core in a highly nonlinear PCF. (Source: http://www.blazephotonics.com)

To obtain a small beam spot at the focus of L1, about the size of the PCF core, a beam expander is integrated in the system to collimate and expand the beam diameter. An aspheric with 8 mm focal length and 0.50 NA couples the laser into the PCF input face. At the fiber end is another aspheric which guides the output pulses towards the entrance slit of a monochromator/ streak camera.

The PCF is a highly nonlinear fiber from BlazePhotonics. Its core diameter of 2.3 mm is designed for zero-dispersion wavelength at 790±5 nm. The 50 and 100 cm PCFs have their ends cleaved clean to minimize reflection losses especially at the input face. The PCF was attached to an *xyz* stage, which offers a great deal of freedom over positioning the input end at the focus of L1. Scanning electron microscopy (SEM) photos of the core and cladding structures of a highly nonlinear PCF are shown in Fig. 2.

RESULTS AND DISCUSSION

The input and output spectra of femtosecond pulses in a 50 cm PCF is shown in Fig. 3. It features a series of spectra arranged according to increasing input pump power P_o. We had observed that an incremental increase with P_o yields a spectrum containing several orders of side lobes. However, we concede that the increased complexity of the featured side lobes cannot be solely attributed to the increase in P_o. The corresponding change in the pump polarization when varying P_o was observed to affect the coupling efficiency on the fiber input. Apparently, however, Figs. 3(b)–3(d) highlight

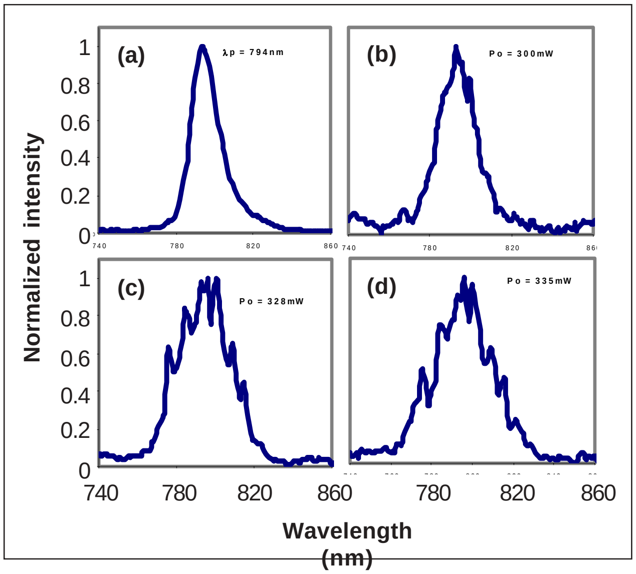

Fig. 3. Input and output spectra measured using a mochromator on a 50 cm PCF for different pump powers: (a) Input pump, λ_p = 794 nm, (b) P_o = 300 mW, (c) P_o = 328 mW, and (d) P_o = 335 mW.

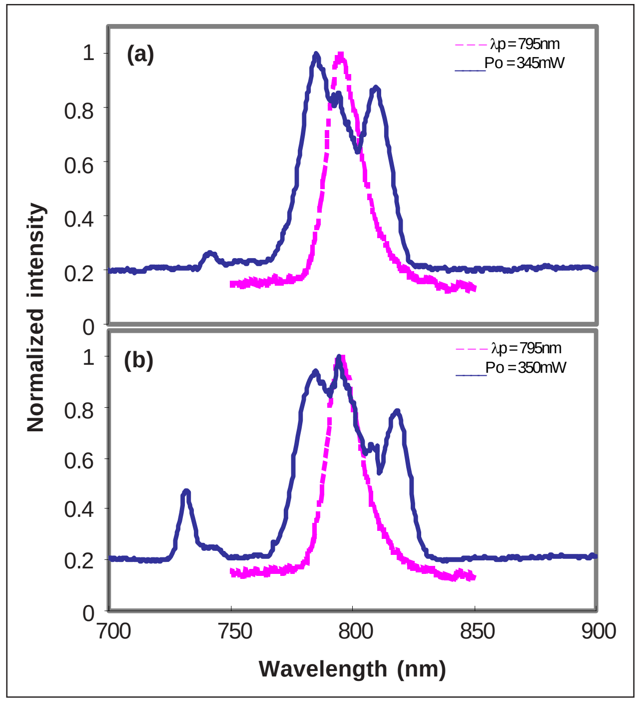

Fig. 4. Input and output spectrum measured on a 100 cm PCF pumped at 795 nm for different pump powers: (a) 345 and (b) 350 mW.

that the peak wavelength of each side lobe is insensitive to the input power. Although spectral details are added with increasing P_o, the unique locations of the side lobes are retained. Some authors suggest that the characteristic asymmetries in the lobe are due primarily to intrapulse Raman scattering, a crucial factor in the route towards SCG.

Figure 4 above shows the output spectra of measurements made on a 100 cm PCF pumped at 795 nm. The spectrum of the input pump is embedded on each figure for the purpose of clarity. Broadening of the spectrum is induced by Raman scattering (RS). As P_o increases, considerable shifting of the pulse towards the infrared region is observed. This is a result of Raman-induced soliton self-frequency shift. Consequently, with increasing P_o energy is efficiently transferred towards shorter wavelengths. New peaks have started to emerge at the region of shorter wavelengths. For an input power of 350 mW, a distinctly intense pulse appers at 732 nm. This dispersive waves accumulate energy as higher-order solitons are generated and shift towards longer wavelengths.

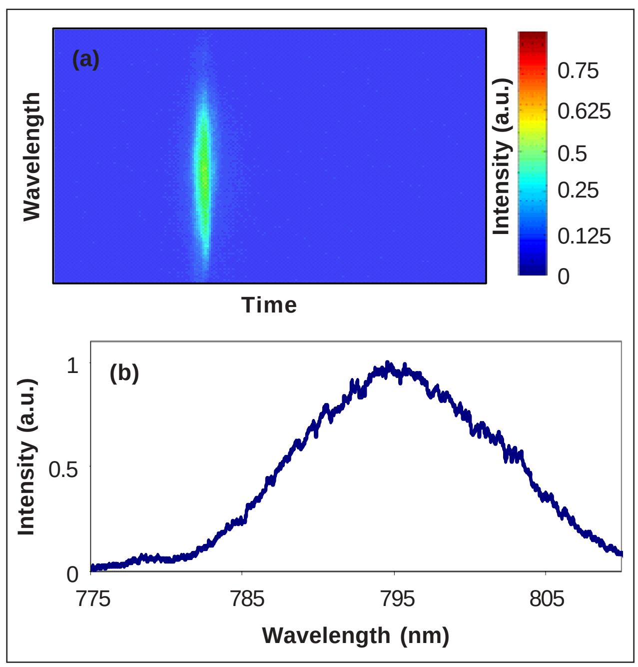

Fig. 5. (a) Spectrogram of the input pulse captured by a streak camera. (b) spectral profile of the input pulse.

Spectrograms of both input and output pulses from a 50 cm PCF are shown in Figs. 5 and 6. The input pump is centered at 795 nm.

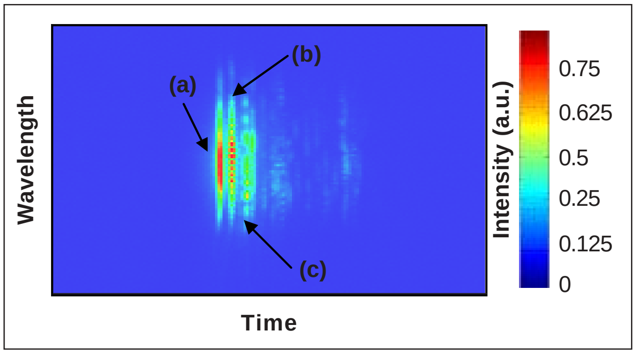

Fig. 6. Spectrogram of the output pulse reveals decomposition of the input into different modes.

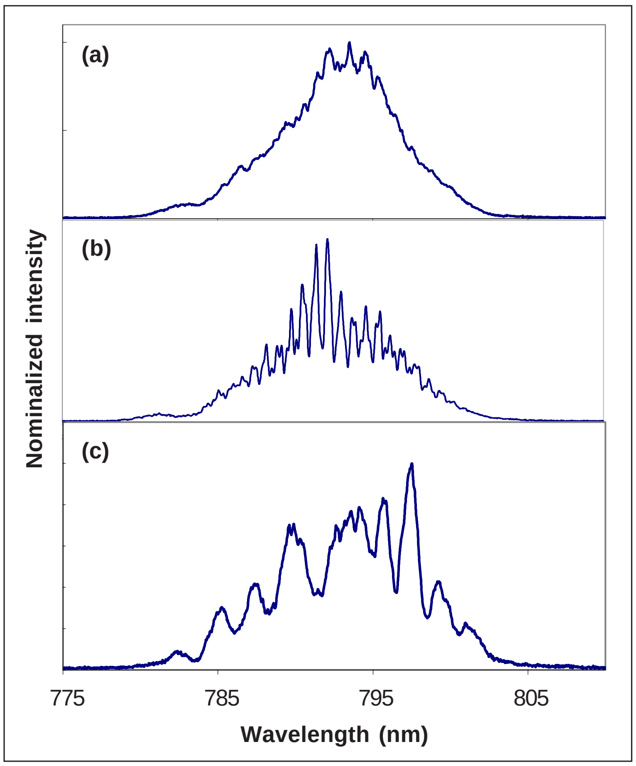

Fig. 7. (a)–(c) Measured spectrum of the modes indicated by the arrows in Fig. 6.

The pump spectrum in Fig. 5(b) assumes a broad Gaussian envelope which extends from 775 to 810 nm. Meanwhile, the spectrogram of the output pulses (Fig. 6) features a number of modes exhibiting different spectral profiles. The spectrogram of the output pulse shows that each of these modes evolve quite independently of each other. Featured in Figs. 7(a)–7(c) are three of the output modes. Each mode has generally narrower spectrum as compared with the pump. Integrating the spectrum of all measured modes will reveal that each individual mode is summarily a decomposition of the input pump.

CONCLUSION

Trains of ~100 fs pulses at 794 and 795 nm are launched into 50 and 100 cm solid-core PCFs. The output spectrum of the 50 cm PCF measured by a monochromator reveals asymmetric side lobes induced through intrapulse Raman scattering. The measured spectrum from a 100 cm PCF pumped at 795 nm shows an emergence of a dispersive wave peaked at 732 nm as a result of Raman-scattering-induced soliton self-frequency (SSF) shift. RS and SSF have also been observed to lead to spectral broadening of the pump. The spectrogram of the 50 cm PCF captured by a streak camera shows decomposition of the input pump into different modes.

REFERENCES

Agrawal, G.P., 1995. Nonlinear fiber optics. 2nd ed. Academic, New York.

Cristiani, I., R. Tediosi, L. Tartara, & V. Degiorgio, 2004. Dispersive wave generation by solitons in microstructured optical fibers. *Opt. Express*. **12**: 124 – 135.

Gaeta, A., 2002. Nonlinear propagation and continuum generation in microstructured optical fibers. *Opt. Lett*. **27**: 924–926.

Genty, G., M. Lehtonen, H. Ludvigsen, J. Broeng, & M. Kaivola, 2002. Spectral broadening of femtosecond pulses into continuum radiation in microstructured fibers. *Opt. Express*. **10**: 1083–1098.

Genty, G., M. Lehtonen, H. Ludvigsen, & M. Kaivola, 2004. Enhanced bandwidth of supercontinuum generated in microstructured fibers. *Opt. Express*. **12**: 3471–3480.

Knight, J.C., 2003. Photonic crystal fibers.*Nature*. **424**: 847–851.